TOBACCO MOSAIC VIRUS-SUPPORTED SILICON ANODE FOR LITHIUM-ION BATTERIES

Xilin Chen[a], Konstantinos Gerasopoulos[b,c,e], Juchen Guo[a], Reza Ghodssi[b,c,d,e], James N. Culver[f], Chunsheng Wang[a, *]

[a]Department of Chemical & Biomolecular Engineering, [b]MEMS Sensors and Actuators Laboratory (MSAL), [c]Department of Electrical and Computer Engineering, [d]Institute for systems Research (ISR), [e]Department of Materils Science and Engineering, [f]Center for Biosystems Research, Univeristy of Maryland Biotechnology Institute, University of Maryland College Park, MD 20742

Abstract: A novel three-concentric-layer nano-sized silicon anode has been fabricated by employing the *Tobacco mosaic virus.* These three layers are the innermost *Tobacco mosaic virus*, the middle nickel current collector, and the outermost silicon active material. Because the nano-materials provide higher plasticity and deformability to accommodate the extreme volume charge, this novel silicon anode structure has a very high capacity (3300mAh/g), excellent charge-discharge rate capability, and exceptional cyclic life, 2000mAh/g capacity retention after 150 cycles at 1C charge-discharge rate.

Keywords: Silicon anode, lithium-ion battery, Tobacco mosaic virus, Sputtering, Nano-structure

INTRODUCTION

Silicon is a potential anode material for lithium-ion batteries due to its highest theoretical capacity of 3572 mAh/g [1]. However, the significant volume change (270%) during lithium ion insertion/extraction makes the capacity of the silicon anode fade very fast [2]; this is the primary reason that prevents its use in practical applications despite its high capacity. The *Tobacco mosaic virus* (TMV) is a high aspect ratio cylindrical plant virus with a length of 300 nm, an outer diameter of 18 nm, and an inner diameter 4 nm. Genetically modifying the virus to introduce cysteine residues (amino acid with thiol groups), in its coat proteins, enables patterning of the TMV particles onto metal surfaces as well as enhanced metal coating in electroless plating solutions due to strong, covalent-like interactions between the thiol groups of the cysteines and metal ions [3].According to our study, nickel-coated TMV1cys (a virus mutation with one cysteine residue in each coat protein subunit) bio-templates have a three-dimensional nanostructure and high surface area [4]. They have been used to develop micro-fabricated nickel-zinc micro-batteries [5]. It is expected that this 3-D nanostructure can accommodate the volume change of the silicon anode during lithium ion insertion/extraction and enhance the cycle stability. Therefore, nickel-coated TMV1cys bio-templates are used to fabricate silicon anodes for lithium-ion batteries.

EXPERIMENTAL

The silicon anode is synthesized by sputtering in an argon atmosphere onto the nickel-coated TMV template forming a nickel/core-silicon/shell 3-D geometry structure. The synthesis process begins with the TMV1cys self-assembly during which pre-cleaned stainless steel discs are immersed in a TMV1cys solution with a concentration of 0.1 g/L in 0.1M PH 7 sodium phosphate buffer for 48 hours to allow adequate virus attachment onto the metal surfaces. The next step involves the activation process of the TMV1cys with palladium catalytic clusters via the reduction of Pd^{2+} to Pd^0 on the cysteine residue locations using a hypophosphite reducing agent. Following this process, nickel is deposited on the virus surface in an electroless plating bath. The activated TMV1cys templates are put into a nickel solution for 5 minutes with the presence of $(CH_3)_2NHBH_3$ (Dimethylamine borane, DMAB) reducing agent. After nickel deposition, the samples are dried overnight in a vacuum oven at 120°C to evaporate any water left on the surface and avoid oxidation. Finally, sputtering deposition in an AJA sputtering system is used to realize the silicon anode. The process is performed in a RF mode with a power of 200 W, an argon gas flow of 20 sccm and a chamber pressure of 5 mTorr. The distance between the silicon target and the virus-coated steel disk substrates was set to approximately 110 mm and the chuck was rotated to achieve better uniformity. To estimate the silicon loading which is the parameter of interest for capacity calculations, the mass of every disc is weighed with a high precision microbalance (Mettler Toledo, XS105 dualRange) with an accuracy of 1μg before and after silicon deposition.

The TMV/Ni/Si covered discs are assembled into coin cells (R2032) in an argon-filled glove box, using lithium foil as a counter electrode and a 1M LiPF$_6$ solution as electrolyte. An Arbin BT-2000 battery test system with computer-operated software is used to conduct the experiments and record the data.

A Hitachi SU-70 HR-SEM with EDS was used to observe the anode 3-D structure and analyze the elements in the silicon anode.

RESULTS AND DISCUSSION

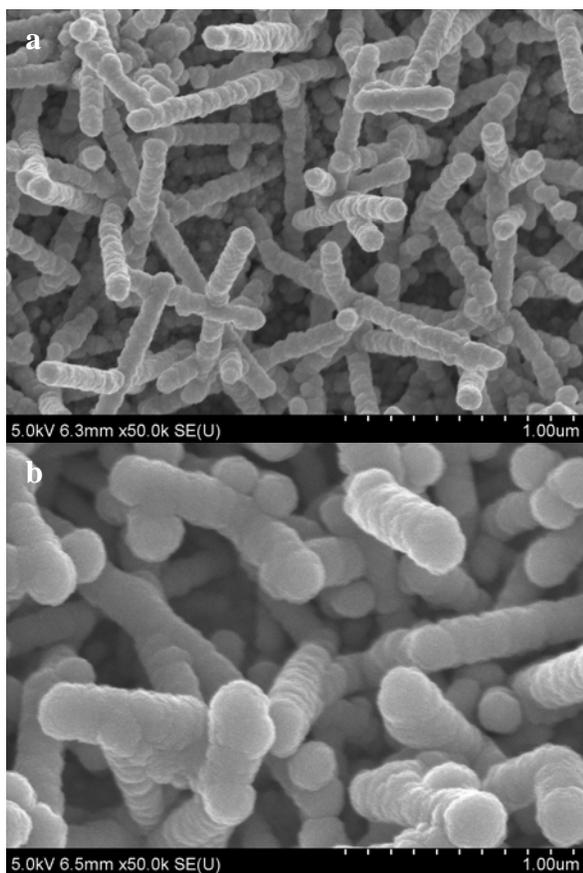Shown in Figure 1 are SEM images before and after silicon deposition while figure 2 shows the

Figure 1 a) Nickel coated TMV1cys bio-template b) Silicon coated anode for lithium-ion battery

elemental analysis of one nano-post shown in figure 1b. As Shown in figure 1a, the nickel coated TMV1cys are near-vertically aligned on the stainless steel disc surface. After silicon deposition, the diameter of the TMV1cys grows from 100 nm to about 200 nm (shown in figure 1b). The EDS spectrum figure 2 shows some oxygen exists in the
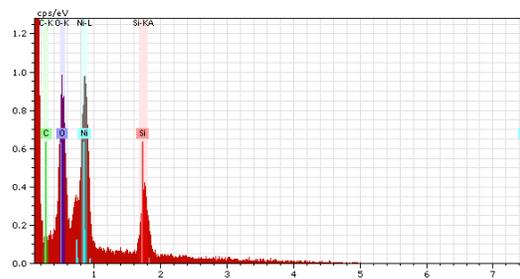

Figure 2 Elemental analysis of the silicon coated TMV1cys bio-template

anode except silicon and nickel. The oxygen may be introduced during transportation by adsorption or/and partial oxidization of silicon.

Shown in figure 3 is the relationship of the silicon load on the TMV1cys templates and control surface (thoroughly cleaned stainless steel disc) and the sputtering time. It is clear that the silicon load on the TMV1cys templates is about 50% higher than that on the control surface. This is because the nickel coated TMV1cys templates are nano-sized and have much larger surface than the control surfaces.

This novel silicon anode has unique nickel/core-silicon/shell nanoarchitecture. With the nickel metal core, every nano-sized silicon post (shown in figure 2b) is directly connected to the current collector, a stainless steel disc, and able to contribute to the capacity of the anode. This explains why this TMV-supported anode has a very high initial capacity close to the theoretical value of 3572 mAh/g (as shown in
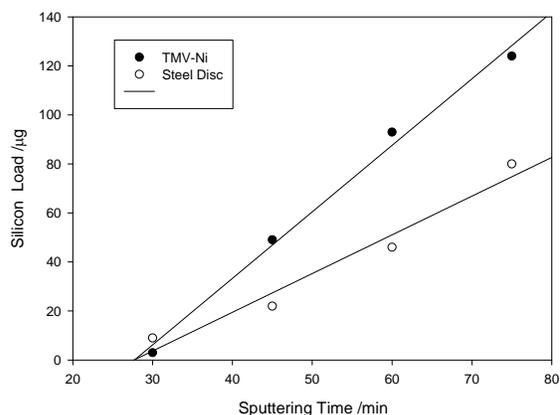

Figure 3 Silicon load on the TMV1cys template and control surface

figure 4) at 1/3C (1C=2000mAh/g) charge rate.

Shown in figure 5 are the cyclic life performances of TMV1cys-supported silicon anode and silicon on
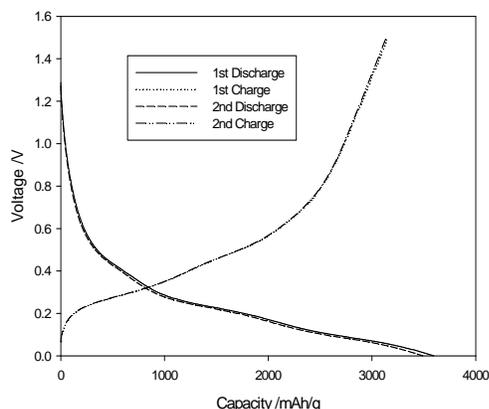
Figure 4 The first two cycle profiles of the Silicon anode supported by TMV template at C/3 rate
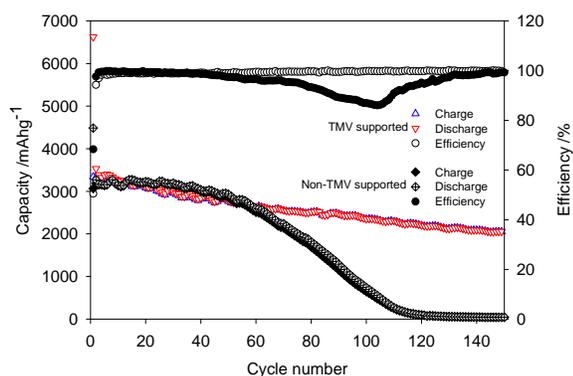

Figure 5 Cyclic performances of TMV1cys- and non-TMV1cys- supported silicon electrodes

control surface at 1C charge-discharge rate during the 0-1.5V potential range. Both silicon anodes have similar capacity within the first 50 cycles. After this point, the capacity of the silicon anode on the control surface starts fading fast. From the figure, it can be seen that the coulombic efficiency, which is defined as a ration of charge capacity to discharge capacity, decreases from nearly 100% to 80% for silicon on control surfaces, while the coulombic efficiency of the TMV1cys-supported silicon electrode stay around 100%. After 120 cycles, the capacity of silicon on the sample without TMV1cys becomes extremely low, almost zero. This fast fading is due to the pulverization of silicon film on the control surface caused by extreme volume change during lithium insertion and extraction. The pulverized silicon particle is disconnected from the current collector and cannot contribute to the capacity any more. However, the capacity of TMV1cys-supported silicon anode decreases very slow, about 0.25% per cycle. After 150

cycles, the retention of the capacity is still more than 2000mAh/g. The excellent cyclic life performance and capacity of TMV1cys-supported silicon anode originates from its unique core-shell structure. First of all, the strong bonds between TMV1cys and nickel make the nano-posts flexible to avoid pulverization during lithium insertion and extraction. Secondly, the structure of the electrode is truly nano-sized and offers higher plasticity and deformability [6-8] to accommodate the extreme volume change during lithiation and delithiation process. A third factor is related to the spaces among the posts, as show in figure 1b, which also help to accommodate the volume expansion during lithium insertion. Finally, the inner nickel post in every silicon post is directly connected to the current collector, the stainless steel substrate, and also acts as a part of current collector. This means every silicon post has its own current collector and is able to contribute to total capacity of the electrode and explains why the initial capacity of the TMV1cys supported silicon electrode is very close to the theoretical value at C/3 charge-discharge rate. However, the pulverization of silicon electrode is only alleviated by TMV1cys-supported structure but
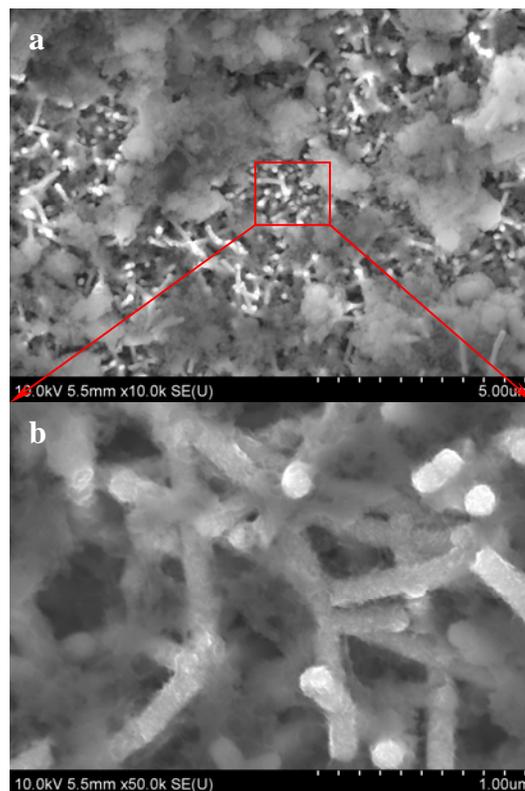

Figure 6 SEM images of TMV1cys-supported silicon electrode after performance test

cannot be eliminated completely. Thus, the capacity of the silicon electrode still decreases slowly.

The TMV1cys supported electrode structure after performance test (150 cycles) is also studied by SEM. As shown in figure 6a, a significant amount of solid electrolyte interface (SEI) film is found on the top of the electrode. At a large magnification (as shown in figure 6b), it can be seen that every silicon post is also covered by the SEI film and maintains the same structure as before the performance tests as shown in figure 1. This explains why the capacity of TMV1cys-supported silicon anode has a better cyclic life performance than that on control surface.

CONCLUSION

The TMV1cys-supported silicon anode reported here has an exceptional three-dimensional nanostructure. The silicon posts in this electrode are well patterned on the stainless steel disc. The truly nano-sized structure provides higher plasticity and deformability to accommodate the extreme volume change during lithiation and delithiation process. After repeated cycling experiments, no obvious degradation in the structure of the electrode was observed while high capacity retention of ~70% (comparing to the charge capacity of second cycle) in the potential range of 0 to 1.5 V was achieved. These results, combined with the simplicity of the TMV self-assembly and patterning create new opportunities for the utilization of inexpensive and versatile synthesis techniques for energy-storage applications.

ACKOWNLEDGEMENTS

REFERENCES

[1] S. Cahen, R. Janot, L. Laffont-Dantras, and J.M. Tarascon, 2008, Chemical reaction of $SiCl_4$ for the preparation of silicon-graphite composites used as negative electrodes in lithium-ion batteries, *Journal of The Electrochemical Society*, 155 (7) A512-A519

[2] C. K. Chan, H. Peng, G. Liu, K. MclLWRATH, X. Zhang, R. A. Huggins, and Y. Cui, 2008, High-performance lithium battery anodes using silicon nanowires, *Nature nanotechnology*, 3 31-35

[3] S. Lee, E. Royston, J. N. Culver, and M. T. Harris, 2005, Improved metal cluster deposition on a genetically engineered tobacco mosaic virus template, *Nanotechnology* 16, S435-S441

[4] E. Royston, A. Ghosh, P. Kofinas, M. T. Harris, and J. N. Culver, 2008, Self-assembly of virus-structured high surface area nanomaterials and their application as battery electrodes, *Langmuir*, 24 (3) 906-912

[5] K. Gerasopoulos, M. McCarthy, E. Royston, J. N. Culver, and R. Ghodssi, 2008, Nanostructured nickel electrodes using the Tobacco mosaic virus for microbattery applications, *Journal of Micromechanics and Microengineering*, 18 104003 (8pp)

[6] I. Chen and L. Xue, 1990, Development of Superplastic Structural Ceramics, *Journal of American Ceramic Society*, 73, 2585

[7] H. Gleiter, 1989, Nanocrystalline materials, *Progress in Materials Science*, 33 223

[8] H. Li, X. Huang, L. Chen, Z. Wu, and Y. Liang, 1999, A High Capacity Nano-Si Composite Anode Material for Lithium Rechargeable Batteries, *Electrochemical and Solid-State Letter*, 2 (11) 547-549

*Corresponding author: Chunsheng Wang, Ph.D,
Email: cswang@umd.edu Phone: (301)405-0352